Strong electrical magneto-chiral anisotropy in tellurium

G. Rikken, N. Avarvari

Strong electrical magneto-chiral anisotropy in tellurium

G.L.J.A. Rikken

Laboratoire National des Champs Magnétiques Intenses
UPR3228 CNRS/EMFL/INSA/UGA/UPS, Toulouse & Grenoble, France.

N. Avarvari
MOLTECH-Anjou, UMR 6200, CNRS, UNIV Angers,
2 blvd Lavoisier, 49045 ANGERS Cedex, France

(Dated: May 13, 2019)

We report the experimental observation of strong electrical magneto-chiral anistropy (eMChA) in trigonal tellurium (t-Te) crystals. We introduce the tensorial character of the effect and determine several tensor elements and we propose a novel intrinsic bandstructure-based mechanism for eMChA which gives a reasonable description of the principal results.

Chirality is important in many areas of physics, chemistry and biology, where objects or materials can exist in two non-superimposable forms, one being the mirror image of the other (enantiomers). Such a system is not invariant under parity reversal. If in addition it is not invariant under time-reversal because it has a magnetization, an entire class of effects called magneto-chiral anisotropy (MChA) becomes allowed. The existence of MChA in the optical properties of chiral systems under magnetic field has been predicted since 1962 [1],[2],[3],[4],[5]. It corresponds to a difference in the absorption and refraction of unpolarized light propagating parallel or anti-parallel to the magnetic field in a chiral medium. After its first experimental observations [6],[7],[8], its existence was confirmed across the entire electromagnetic spectrum, from microwaves [9] to X-rays [10]. The existence of MChA was further generalized to other transport phenomena [11]. It was experimentally observed in the electrical transport in bismuth helices [11], carbon nano tubes [12], [13] and bulk organic conductors [14], as an electrical resistance R that depends on the handedness of the conductor and on the relative orientation of electrical current $\mathbf{I}$ and magnetic field $\mathbf{B}$: $R^{D/L}(\mathbf{B},\mathbf{I}) = R_0(1+\mu^2B^2+\gamma^{D/L}\mathbf{B}\cdot\mathbf{I})$, with $\gamma^D = -\gamma^L$ referring to the right- and left-handed enantiomer of the conductor. More recently, such electrical MChA was also observed in chiral magnetic systems [15],[16],[17], which was tentatively explained by scattering by chiral spin fluctuations. The spin filter effect [18] can also be regarded as a form of eMChA. As another generalization, MChA was recently observed in the propagation of ultrasound [19]. Although the characteristics of eMChA make it interesting for applications, the small values reported so far daunt their development. Whereas a microscopic theory exists for optical MChA [5], apart from some simplified model calculations [20], no quantitative theory exists for eMChA in bulk materials. Here we report the experimental observation of much larger values in t-Te, and introduce a novel intrinsic mechanism for eMChA that explains this observation and allows to identify other materials showing a strong effect.

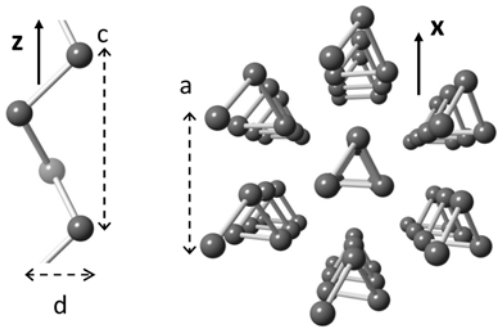

FIG. 1: Trigonal tellurium crystal structure. Left: view on the x-z plane of a single helix. Right: view on the x-y plane. a = 445 pm, c = 593 pm, d = 238 pm

Chiral t-Te is an ideal material to study eMChA. It is a well-characterized direct gap semiconductor (E_g = 0,33 eV), with its conduction band minimum and valence band maximum at the H-point in the Brillouin zone. It is intrinsic and non-degenerate at room temperature with a carrier density N around 10^{22} m^{-3}. Its crystal structure consists of parallel stacked helices of 3 Te atom per turn (Fig. 1) and belongs to the crystal class **32.** The chirality of t-Te and the absence of time reversal symmetry at the H point allow for the existence of linear **k**-terms in the bandstructure (**k** = wavevector) [21]. Using this bandstructure, several chiroptical properties (see [22] and references therein) and magneto-optical properties (see [23] and references therein) of t-Te have been calculated, in good agreement with experiment. The existence of a strong eMChA in t-Te is plausible because of its helical crystal structure, and it is further supported by the recent observation of current-induced shifts in the ^{125}Te NMR frequency in t-Te [24]. This observation confirms the existence of strong inverse eMChA in in this material. This effect corresponds to a current induced longitudinal magnetization present in all chiral conductors [11] and therefore implies the existence of a strong

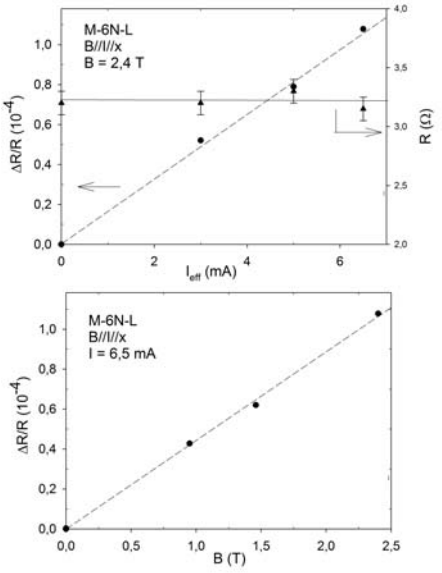

FIG. 2: Current and magnetic field dependence of the resistance (triangles, defined as $R = V^{\omega}/I^{\omega}$) and eMChA (balls, for definition see text) of a x-oriented left-handed Te crystal at 300 K and with a cross section of 5 10^{-7} m^2. Lines are linear fits.

eMChA in t-Te. Theoretical work has addressed several contributions to the inverse eMChA in t-Te (see [25] and references therein) but cannot be straightforwardly adapted to make quantitative predictions for the direct eMChA effect.

Single crystals of zone refined t-Te (purity better than 99,9999%) were commercially obtained [27]. They can be easily cleaved along the c-axis, and etching the cleavage surface with hot concentrated sulfuric acid reveals characteristic etch pits from which the crystal axis orientation and the crystal handedness can be straightforwardly deduced [28]. Typical sample sizes are cross-sections of 0,5 x 0,5 mm^2 and lengths of 4 mm. Gold contacts for colinear 4-terminal resistance measurements were deposited by sputtering and a 200 Hz AC current I^{ω} was injected with a low-distorsion current source. The generated voltages V^{ω} and its second harmonic $V^{2\omega}$ were measured by phase-sensitive detection.

The above expression for $R^{D/L}$ is a simplification, only strictly valid in cubic crystals or isotropic media. In crystals of lower symmetry, the correct description of eMChA requires a fourth rank tensor $\boldsymbol{\gamma}$:

$$E_i^{2\omega} = \gamma_{ijkl}^{D/L} J_j^{\omega} J_k^{\omega} B_l \qquad (1)$$

where $\gamma_{ijkl}^{D} = -\gamma_{ijkl}^{L}$ and J is the current density. The crystal symmetry imposes further restrictions on the tensor components (see e.g. [26]). In the geometry used in our experiments, $i = j = k$ and the cases for $i = x$ and $i = z$ have been addressed by using crystals of different cuts. It can be easily shown that eMChA, defined as $(R(B,I) - R(B,-I))/(R(B,I) + R(B,-I)) \equiv \Delta R/R$ equals $4V^{2\omega}/V^{\omega}$ (for details see [14]-[17]). By taking the difference between the results for $+B$ and $-B$, all nonlinearities that are even in magnetic field are eliminated. The dependence of $\Delta R/R$ on current and magnetic field for an x-oriented left-handed crystal (space group D_3^6) is shown in Figure 2, confirming the strictly linear dependence of eMChA on these quantities. By making different crystal cuts and by rotating the crystals, different tensor components can be measured, as illustrated in Fig. 3 and 4. The enantioselectivity of

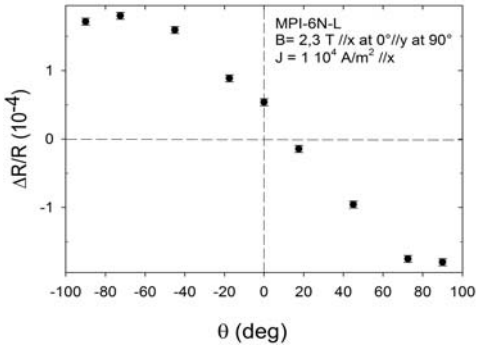

FIG. 3: eMChA of a x-oriented left handed crystal at room temperature, as a function of the angle between **B** and the crystal x-axis. At $\theta = 0°$, $\Delta R/R \propto \gamma_{xxxx}$, at $\theta = \pm 90°$, $\Delta R/R \propto \gamma_{xxxy}$.

the eMChA is illustrated in Figure 4, which shows eMChA results for a left-handed and a right handed crystal (space group D_3^4) in the same orientation, with opposite results. From Figs. 3 and 4 we deduce $3\gamma_{xxxx} \approx \gamma_{xxxy}$,

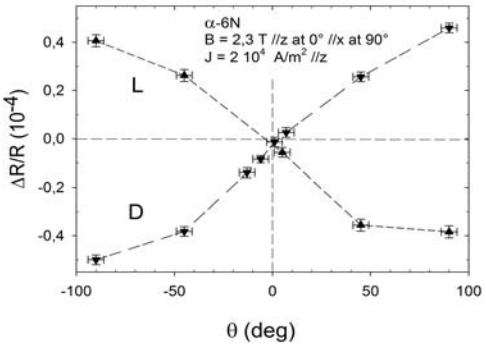

FIG. 4: eMChA of a left-handed (▲) and right-handed (▼) z-oriented Te crystal at room temperature, as a function of the angle between **B** and the crystal z-axis. At $\theta = 0°$, $\Delta R/R \propto \gamma_{zzzz}$, at $\theta = \pm 90°$,$\Delta R/R \propto \gamma_{zzzx}$.

$12\gamma_{zzzx} \approx \gamma_{xxxy}$ and $\gamma_{zzzz} \ll \gamma_{zzzx}$. The latter result does not mean that $\gamma_{zzzz} = 0$, as there is no symmetry argument that imposes that. The uncertainty in the exact geometrical shape of the sample, in combination

with the small value of γ_{zzzz} and the much larger values of the other tensor elements, make it difficult to determine a significant value for this quantity. Fig. 5 shows the temperature dependence of eMChA in the intrinsic regime around room temperature. Table 1 gives

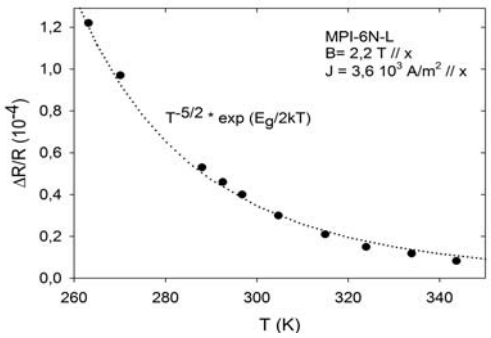

FIG. 5: Temperature dependence of eMChA of an x-oriented left handed crystal. For dotted line, see text.

a summary of the values reported so far for eMChA, illustrating that t-Te shows by far the strongest effect.

Material	γ $[m^2/T \cdot A]$	**Ref.**	**Remark**
t-Te $xxxy$	10^{-8}	this work	RT
TTF-ClO_4	10^{-10}	[14]	RT
$CrNb_3S_6$	10^{-12}	[17]	magnetic, LT
MnSi	$2\ 10^{-13}$	[15]	magnetic, LT
SWCNT	10^{-14}	[12]	LT

Table 1 Summary of published eMChA results (RT room temperature, LT low temperature)

We propose as explanation for the observed eMChA the **k**-linear terms in the t-Te bandstructure around the H-point. Nakoa *et al* [29] have shown theoretically and experimentally that these terms lead to the lifting of the energy degeneracy between valence band states with **k** and **-k** in the presence of a magnetic field perpendicular to the z-axis, whereas as no degeneracy lifting occurs for a magnetic field parallel to the z-axis. Although these authors did not comment on this aspect, such an energy-splitting has to be enantioselective in order to be symmetry allowed. We can therefore heuristically simplify their findings to the existence of a MChA energy term around the t-Te valence band maximum of the form $\Delta\epsilon_v = \chi^{D/L}\mathbf{k}\cdot\mathbf{B}_\perp$ with $\chi^D = -\chi^L$ and $|\chi| \approx 1.5\cdot 10^{-30}\ Jm/T$. A similar behavior was later found for the t-Te conduction band [30]. If we neglect the regular non-parabolicity of the valence band, its energy dispersion relation around the H-point is $\epsilon(\mathbf{k}) = \hbar^2\mathbf{k}^2/2m^* + \chi^{D/L}\mathbf{k}\cdot\mathbf{B}_\perp$. In the constant relaxation time approximation, the Boltzmann equation gives for the electrical conductivity σ [31]:

$$\sigma_{ii} = \frac{q^2\tau}{4\pi^3\hbar^2}\int\left(\frac{\partial\epsilon(\mathbf{k})}{\partial k_i}\right)^2\frac{\partial f}{\partial\epsilon}d^3\mathbf{k} \qquad (2)$$

where f is the distribution function, q the charge, τ the scattering time, m^* the effective mass and for Maxwell-Boltzmann statistics, $\partial f/\partial\epsilon = -f/k_BT$. Applying the magnetic field in the x-direction and neglecting terms in B^2 this results in

$$\sigma_{xx} = \frac{Nq^2\tau}{m^*} - \frac{q^2\tau\chi^{D/L}B}{4\pi^3 m^* k_B T}\int k_x f d^3\mathbf{k} \qquad (3)$$

$$= \sigma_0\left(1-\gamma^{D/L}_{xxxx}J_xB\right) \qquad (4)$$

where

$$\gamma^{D/L}_{xxxx} = m^*\chi^{D/L}/Nq\hbar k_BT \qquad (5)$$

Note that at room temperature an analogous contribution to eMChA will come from the conduction band which, depending on the relative signs of χ for the two bands, may have the same or opposite sign. This electron contribution will disappear at low temperature when t-Te becomes extrinsic p-type. This simple model leads to several predictions:
1) as a general rule, metals, with their much larger carrier density, will show smaller eMChA than semiconductors and semi-metals, in agreement with the table above.
2) for t-Te at 300 K, $\Delta R/R(\mathbf{B}//\mathbf{J}//\mathbf{x}) = \gamma_{xxxx}JB$ with $\gamma_{xxxx} \approx 6.10^{-10}\ m^2A^{-1}T^{-1}$ whereas our experimental result (Fig. 3) gives $\gamma_{xxxx} \approx 2.10^{-9}\ m^2A^{-1}T^{-1}$, a reasonable agreement in view of the simple model.
3) $\gamma_{iiiz} = 0$ in t-Te because of the absence of the degeneracy lifting for $\mathbf{B} \parallel \mathbf{z}$, in agreement with our observations. Other mechanisms for eMChA [11], not included in our model, may still lead to a small non-zero value. One may obtain an estimate for γ_{zzzz} from the free-electron-on-a-helix model [20]. This can only give an upper limit, as there is significant coupling between adjacent Te helices and charge carriers are therefore not confined to one helix. For the same parameters as in Fig. 4, this model predicts $\Delta R/R \approx 10^{-9}$, consistent with the experimental result.
4) Taking into account the temperature dependence of the carrier concentration [31], Eq. 5 implies the temperature dependence of γ_{xxxx} to be $T^{-5/2}\exp(E_g/2k_BT)$. Fig. 5 shows that this is a reasonably good description.
Although t-Te is topologically trivial, the existence of **k**-linear terms in its bandstructure and its strong spin-orbit interaction suggest a link to topological insulators and Weyl semi-metals. Indeed, strong eMChA was also claimed for topologically non-trivial systems like Weyl semi-metals [32] and non-centrosymmetric Rashba superconductors [33], although these systems are not chiral in the strict sense of the term. In line with this suggestion,

t-Te is predicted to become a strong topological insulator under pressure [34] and ARPES measurements have revealed Weyl nodes at ambient pressure [35].
It will be clear that a more sophisticated theoretical approach, including the effect of the Lorentz force, plus the full details of the band structure are necessary to obtain full understanding of eMChA in t-Te and to arrive at an accurate description of all its tensor elements. Our model allows to identify the major contributing factors and allows to identify other materials showing strong eMChA through straightforward band structure calculations, thereby opening a venue for realistic applications of this effect. Obvious candidates are trigonal selenium and its binary alloys with tellurium, and cinnabar ($\alpha-$HgS) that have the same crystal structure, albeit slightly different band structures. At different band structure extrema, the MChA energy term, present around the H point in t-Te, may be zero, which could lead to a much lower eMChA.
In summary, we have experimentally observed strong eMChA in t-Te, we have demonstrated the tensorial character of this effect and we have identified a novel intrinsic bandstructure mechanism that agrees with these results.

This work was supported by the French National Agency for Research (ChiraMolCo, ANR 15-CE29-0006-02).

[1] M.P. Groenewege, Mol. Phys. **5**, 541 (1962).
[2] D.L. Portigal and E. Burstein, J. Phys. Chem. Solids **32**, 603 (1971).
[3] N.B. Baranova, Yu. V. Bogdanov, B. Ya. Zeldovich, Opt. Commun. **22**, 243 (1977).
[4] G. Wagnière and A. Meier, Chem. Phys. Lett. **93**, 78 (1982).
[5] L. D. Barron and J. Vrbancich, Mol. Phys. **51**, 715 (1984).
[6] G.L.J.A. Rikken and E. Raupach, Nature **390**, 493 (1997).
[7] P. Kleindienst and G. Wagnière, Chem. Phys. Let. **288**, 89 (1998).
[8] G.L.J.A. Rikken and E. Raupach , Phys. Rev. **E 58**, 5081-5084 (1998).
[9] S. Tomita, K. Sawada, A. Porokhnyuk, and T. Ueda, Phys. Rev. Lett. **113**, 235501 (2014). Y. Okamura, F. Kagawa, S. Seki, M. Kubota, M. Kawasaki, and Y. Tokura, Phys. Rev. Lett. **114**, 197202 (2015).
[10] M. Ceolín, S. Goberna-Ferrón and J. R. Galán-Mascarós, Adv. Mat. 2012, DOI: 10.1002/adma.201200786, R. Sessoli, M. Boulon, A. Caneschi, M. Mannini, L. Poggini, F.Wilhelm and A. Rogalev, Nat. Phys. **11**, 69 (2015).
[11] G.L.J.A. Rikken, J. Fölling and P. Wyder, Phys. Rev. Lett. **87**, 236602 (2001).
[12] V. Krstić, S. Roth, M. Burghard, K. Kern and G.L.J.A. Rikken, J. Chem. Phys. **117**, 11315 (2002).
[13] J. Wei, M. Shimogawa, Z. Wang, I. Radu, R. Dormaier, and D. H. Cobden, Phys. Rev. Lett. **95**, 256601 (2005).
[14] F. Pop, P. Auban-Senzier, E. Canadell, G. L. J. A. Rikken and N. Avarvari, Nat. Comm. **5,** 3757 (2014).
[15] T. Yokouchi, N. Kanazawa, A. Kikkawa, D. Morikawa, K. Shibata, T. Arima, Y. Taguchi, F. Kagawa, Y. Tokura, Nat. Comm. **8**, 866 (2017).
[16] H. Maurenbrecher, J. Mendil, G. Chatzipirpiridis, M. Mattmann, S. Pané, B. J. Nelson, and P. Gambardella, Appl. Phys. Lett. **112**, 242401 (2018).
[17] R. Aoki,1 Y. Kousaka and Y. Togawa, Phys. Rev. Lett. 122, 057206 (2019).
[18] R. Naaman and D.H. Waldeck Annu. Rev. Phys. Chem. **66**, 263 (2015).
[19] T. Nomura, X.-X. Zhang, S. Zherlitsyn, J. Wosnitza, Y. Tokura, N. Nagaosa and S. Seki, Phys. Rev. Lett. **122**, 145901 (2019)
[20] V. Krstić and G.L.J.A. Rikken, Chem. Phys. Lett. **364**, 51 (2002).
[21] T. Doi, K. Nakao and H. Kamimura, J. Phys. Soc. Japan **28**, 36 (1970).
[22] S. S. Tsirkin, P. Aguado Puente and I. Souza, Phys. Rev. **B 97**, 035158 (2018).
[23] *The Physics of Selenium and Tellurium,* eds. E. Gerland and P. Grosse, Springer 1979.
[24] T. Furukawa, Y. Shimokawa, K. Kobayashi and T. Itou, Nat. Comm. **8**, 954 (2017).
[25] C. Şahin, J. Rou, J. Ma, and D. A. Pesin, Phys. Rev. **B 97**, 205206 (2018).
[26] R.R. Birss, *Symmetry and magnetism*, North Holland (1966).
[27] Alfa Aesar cat. no. 11076.
[28] A. Koma, E. Takimoto and S. Tanaka, Phys. Stat. Sol. **40**, 239 (1970).
[29] K. Nakao, T. Doi and H. Kamimura, J. Phys. Soc. Japan **30**, 1400 (1971).
[30] J. Blinowski, G. Rebmann, C. Rigaux and C. Mysielskci, J. Physique **38**, 1139 (1977).
[31] K.H. Seeger, Semiconductor physics, Springer 1982.
[32] T. Morimoto and N. Nagaosa, Phys. Rev. Lett. **117**, 146606 (2016).
[33] R. Wakatsuki, Y. Saito, S.Hoshino, Y. Itahashi, T. Ideue, M. Ezawa1, Y. Iwasa and N. Nagaosa, Science Adv. **3**, e1602390 (2017).
[34] L. A. Agapito, N. Kioussis, W. A. Goddard III, and N. P. Ong, Phys. Rev. Lett. **110**, 176401 (2013).
[35] K. Nakayama, M. Kuno, K. Yamauchi, S. Souma, K. Sugawara, T. Oguchi, T. Sato, and T. Takahashi, Phys. Rev. **B 95**, 125204 (2017).